Pol. J. Environ. Stud. Vol. 23, No. 4 (2014), 1297-1306

Original Research

Stability Analysis of Rock Mass with Sheet Slope Crack Based on Plates and Shells Theory

Qian Zhang*, Shu-cai Li, Li-ping Li, Qian-qing Zhang, Shao-shuai Shi, Qing-han Wang, Xiang-dong Meng

Geotechnical and Structural Engineering Research Center, Shandong University, Jinan, Shandong 250061, China

Received: 6 March 2013
Accepted: 20 October 2013

Abstract

The application of solid mechanics theory in rock engineering is promoted by the presentation of sheet crack concept and geological model. The special part of rock mass with sheet crack is the problem of structural stability, the failure mechanism of which is different from the structural instability caused by material breakage. First, the rock mass slope with high-steep sheet crack is abstracted into an orthotropic plate to analyze its mechanical forms under different boundary conditions and obtain the non-dimensional buckling critical load of rock mass with sheet crack under different conditions of ratio between thickness and width in the elastic range. Second, the solution toward post-buckling mechanical behaviors of rock mass with sheet crack is processed to obtain the change rules of strength and bearing capacity after buckling, and the analytical solution for post-buckling critical load of rock mass with sheet crack is put forward, providing a new idea for stability analysis of slope and some theoretical reference for similar projects.

Keywords: sheet crack, structural stability, buckling critical load, analytical solution

Introduction

The concept of rock mass with sheet crack systematically adopted by SUN Guang-zhong is that the rock mass generated by interlaminar disturbed cutting or cleavage is provided with the characteristics of sheet crack when the length-thick ratio of rock stratum is greater than 15~18 [1]. This kind of rock mass is cut by a group of penetrating surfaces and has cracking sheet structure with the shape of clintheriform or cataclastic clintheriform. The deformation and damage of rock mass with sheet crack is mainly controlled by weak structural surfaces and also sometimes by penetrating hard structural surfaces. The failure mechanism and mode are the buckling and bending of cracking sheet structure. Buckling failure means that the tabular rock stratum downward slips along the lower weak structural surfaces and then produces arches and is cut off, causing damage at the foot of the slope. For example, the slope height of Bawang Mountain with the composition of limestone is 940 m, and the dip angle of rock is about 40º; the thickness of damaged rock stratum is 15 m, underneath which is a thin clay interlayer. The upper limestone rock stratum produces creep along the lower clay rock stratum and the part near the riverbed at slope foot is bent under the action of gravity, for a long time causing buckling failure. Bending failure is more common in the roof and baseplate damage of an underground cavern; for example, the roof can break away from the upper strata, growing creaks to produce the rock beam. This kind of rock beam can present vertical bending because of its own weight, and when the creaks are produced in the rock beam, the neutral axis will move upward with the gradual outspread of creaks until it runs through the whole beam and then a part of the rock mass loosens and falls [2].

*e-mail: bowanghou1@sina.com

The application of solid mechanics theory in rock engineering is promoted by the presentation of sheet crack concept and geological model, the basic computing methods of which consist of the static method and energy method. The special part of rock mass with sheet crack is the problem of structural stability, the failure mechanism of which is different from the structural instability caused by material breakage. Not all damage to tabular structures is structural instability; for example, it is not appropriate that the bending failure of a tabular structure is called structural instability, the model for which is far from the common continuum model.

At present, many scholars have studied the stability of rock mass with sheet slope crack, making lots of valuable results [3-6]. But the rock mass with sheet slope crack was abstracted into column beam in most studies with mechanical analysis of column beam, and the stability evaluation of which is progressed mainly by the stability theory of struts. In fact, the stability of plates is far away from the stability problem of struts, and the important difference between the buckling of elastic plates and the instability of columns is that the buckling of columns marks the loss of bearing capacity, while the plates can continue to resist the increased pressure after reaching the critical load, and the load can substantially exceed the critical load of plates, so it is necessary for the stability of rock mass with sheet slope crack to be studied by plate-shell theory.

The buckling and post-buckling characteristics of rock mass with sheet slope crack are solved by numerical method based on plate-shell theory in this paper, and then the validation is progressed using the on-site testing data of hazardous rock mass in Zhenziyan.

Buckling Analytical Solution of Orthogonal Various Heterosexual Plates

Research with regard to the stability of thin plates has been carried out at home and abroad, whether the small-deflection or large-deflection buckling are based on the thin pates neglecting transverse shear deformation. In fact, it is necessary to consider the effect of transverse shearing deformation because the increase of wall thickness of plate and shell structures in practical engineering often goes beyond the application of a thin wall. The deformation feature of plate and shell buckling is bending deformation, and the internal force characteristic is consistent with that of large-deflection bending, so the buckling theory widely used in calculation is based on von Karman's large-deflection equations, and the top priority problem to be solved is the critical load of buckling determined by the equilibrium state of buckling. In the small-deflection buckling theory of plate and shell, the stress state before buckling is usually assumed for the non-moment state, making the balance equation of plates linearized [7-11].

On the basis of geometric equations, physical equations and equilibrium equations of medium plates, the displacement governing differential equations of medium plates concerning three independent variables, i.e. one middle surface displacement and two middle surface intersection angles are established, so the displacement governing differential equations of small-deflection buckling of medium plates can be obtained accordingly. Then, the displacement governing differential equations of simply supported rectangular plates are solved by the method of double trigonometric series, and the critical load expression of small-deflection buckling of simply supported rectangular medium plates is obtained by MATLAB. The above-mentioned theory applied in the calculation for force-bearing state of rock mass with sheet slope crack can provide reference for the calculation of slope stability.

Fundamental Relations of Medium Plates [11-13]

The displacement component at any point $P(x, y)$ in the middle surface of medium plates is $w(x, y)$, and the displacement components at any point $P_1(x, y, z)$ in the non-middle surface of medium plates are $u_1(x, y, z)$, $v_1(x, y, z)$, $w_1(x, y, z)$, then the relations of the two points are:

$$u_1 = u + z\phi, \quad v_1 = v + z\psi, \quad w_1 = w \tag{1}$$

...where the middle surface displacements $u = 0$, $v = 0$, ϕ, and ψ are independent angles at any point $P(x, y)$ in the middle surface. Thus, the strains at $P_1(x, y, z)$ can be expressed as:

$$\varepsilon_1^z = \varepsilon_1 + z\kappa_1, \quad \varepsilon_2^z = \varepsilon_2 + z\kappa_2, \quad \omega^z = \omega + z\tau, \\ \varepsilon_{13}^z \approx \bar{\varepsilon}_{13}, \qquad \varepsilon_{23}^z \approx \bar{\varepsilon}_{23} \tag{2}$$

...where the membrane strains in the middle surface of medium plates are:

$$\varepsilon_1 = \frac{\partial u}{\partial x} = 0 \qquad \varepsilon_2 = \frac{\partial v}{\partial y} = 0 \qquad \omega = \frac{\partial v}{\partial x} + \frac{\partial u}{\partial y} = 0 \tag{3}$$

The bending strains in the middle surface of medium plates are:

$$\kappa_1 = \frac{\partial \phi}{\partial x} \qquad \kappa_2 = \frac{\partial \psi}{\partial y} \qquad \tau = \frac{\partial \psi}{\partial x} + \frac{\partial \phi}{\partial y} \tag{4}$$

The transverse shear strains in the middle surface of medium plates are:

$$\varepsilon_{13} = \phi + \frac{\partial w}{\partial x} \qquad \varepsilon_{23} = \psi + \frac{\partial w}{\partial \mathrm{y}} \tag{5}$$

The transverse shears of medium plates are:

$$N_1 = \frac{Gh}{k_\tau}\varepsilon_{13} \qquad N_2 = \frac{Gh}{k_\tau}\varepsilon_{23} \tag{6}$$

And the internal forces of medium plates are:

$$M_1 = D(\kappa_1 + \mu\kappa_2)$$

$$M_2 = D(\kappa_2 + \mu\kappa_1) \tag{7}$$

$$M_{12} = M_{21} = D\frac{(1-\mu)}{2}\tau$$

...where the bending stiffness D = $Eh^3/[12(1-\mu^2)]$, k_T is the conversion factor of the transverse shear strains ε_{13}, ε_{23} and average values of transverse shear strains $\overline{\varepsilon}_{13}$, $\overline{\varepsilon}_{23}$ (the value often takes 1 or 5/6), and the equilibrium equations of medium plates are:

$$\frac{\partial N_1}{\partial x} + \frac{\partial N_2}{\partial y} + T_1\kappa_1 + T_2\kappa_2 + 2T_{12}\tau + q = 0 \tag{8a}$$

$$\frac{\partial M_2}{\partial y} + \frac{\partial M_{12}}{\partial x} - N_2 = 0 \tag{8b}$$

$$\frac{\partial M_1}{\partial x} + \frac{\partial M_{21}}{\partial y} - N_1 = 0 \tag{8c}$$

...where the nonlinear terms in Eq. (8a) are produced because of the large-deflection bending, and the effect of nonlinearity is not considered in the other equations. When the effect of nonlinear terms is neglected, the above equations can degenerate into the fundamental equations of small-deflection bending.

Displacement Governing Differential Equations of the Buckling of Medium Plates

The membrane forces in small-deflection buckling theory of shells are directly produced by the action of in-plane load, which can be regarded as known quantities. When the medium plates are not subjected to normal load (q=0), the fundamental equations of small-deflection buckling of medium plates expressed by displacement components (w, ϕ, ψ) can be obtained:

$$\frac{Gh}{k_\tau}\left[\frac{\partial\phi}{\partial x} + \frac{\partial\psi}{\partial y} + \frac{\partial^2 w}{\partial x^2} + \frac{\partial^2 w}{\partial y^2}\right] + T_1\frac{\partial^2 w}{\partial x^2} + T_2\frac{\partial^2 w}{\partial y^2} + 2T_{12}\frac{\partial^2 w}{\partial x\partial y} = 0 \tag{9a}$$

$$\frac{1-\mu}{2}\frac{\partial^2\psi}{\partial x^2} + \frac{1+\mu}{2}\frac{\partial^2\phi}{\partial x\partial y} + \frac{\partial^2\psi}{\partial y^2} - \frac{1}{D}\left[\frac{Gh}{k_\tau}\left(\psi + \frac{\partial w}{\partial y}\right)\right] = 0 \tag{9b}$$

$$\frac{\partial^2\phi}{\partial x^2} + \frac{1-\mu}{2}\frac{\partial^2\phi}{\partial y^2} + \frac{1+\mu}{2}\frac{\partial^2\psi}{\partial x\partial y} - \frac{1}{D}\left[\frac{Gh}{k_\tau}\left(\phi + \frac{\partial w}{\partial x}\right)\right] = 0 \tag{9c}$$

The transverse shear items $\frac{Gh}{k_\tau}(\phi + \frac{\partial w}{\partial x})$ and $\frac{Gh}{k_\tau}(\psi + \frac{\partial w}{\partial y})$ in Eqs. (9b-9c) are substituted into Eq. (9a), the foundational equation concerning one middle surface displacement component (w) can be obtained. The intersection angles ϕ and ψ are no longer independent variables, i.e. $\phi = -\frac{\partial w}{\partial x}$, $\psi = -\frac{\partial w}{\partial y}$, then:

$$-D\nabla^2\nabla^2 w + T_1\frac{\partial^2 w}{\partial x^2} + T_2\frac{\partial^2 w}{\partial y^2} + 2T_{12}\frac{\partial^2 w}{\partial x\partial y} = 0 \tag{10}$$

...where the Laplace operator is $\nabla^2 = \frac{\partial^2}{\partial x^2} + \frac{\partial^2}{\partial y^2}$. Eq. (10) is the same as Eq. (12.1) in literature [7]. When normal force (q) is zero, the fundamental equation of the plates buckling only subjected to membrane force is the same as Eq. (12.1a) in literature [7] and Eq. (2.2) in literature [8].

Buckling of Simply Supported Rectangular Medium Plates with Unidirectional Pressure

It is assumed that one simply supported rectangular medium plate is subjected to uniform pressure p (Fig. 1). The translation motions of plate edges occur in plane, and the stresses in other directions are not produced by the deformation along the direction of x axis. The membrane forces here are $T_1 = -p$, $T_2 = T_{12} = 0$, so Eq. (10) can be rewritten as:

$$-D\nabla^2\nabla^2 w - p\frac{\partial^2 w}{\partial x^2} = 0 \tag{11}$$

The functions of deflections and angles are expressed by double trigonometric series as:

$$w(x,y) = \sum_{m=1}^{\infty}\sum_{n=1}^{\infty} W_{mn}\sin\frac{m\pi x}{a}\sin\frac{n\pi y}{b} \tag{12a}$$

$$\phi(x,y) = \sum_{m=1}^{\infty}\sum_{n=1}^{\infty} \Phi_{mn}\cos\frac{m\pi x}{a}\sin\frac{n\pi y}{b} \tag{12b}$$

$$\psi(x,y) = \sum_{m=1}^{\infty}\sum_{n=1}^{\infty} \Psi_{mn}\sin\frac{m\pi x}{a}\cos\frac{n\pi y}{b} \tag{12c}$$

$$(m,n = 1,2,3,\cdots)$$

The above equations all satisfy the boundary conditions of four simply supported edges, and W_{mn}, Φ_{mn}, and Ψ_{mn} are undetermined coefficients. Eqs. (12a-12c) are substituted into Eq. (10), and the following equations can be obtained:

$$\frac{Gh}{k_\tau}\left[\left(\frac{m\pi}{a}\right)^2 + \left(\frac{n\pi}{b}\right)^2\right]W_{mn} + \frac{Gh}{k_\tau}\left[\frac{m\pi}{a}\Phi_{mn} + \frac{n\pi}{b}\Psi_{mn}\right] - p\left(\frac{m\pi}{a}\right)^2 W_{mn} = 0 \tag{13a}$$

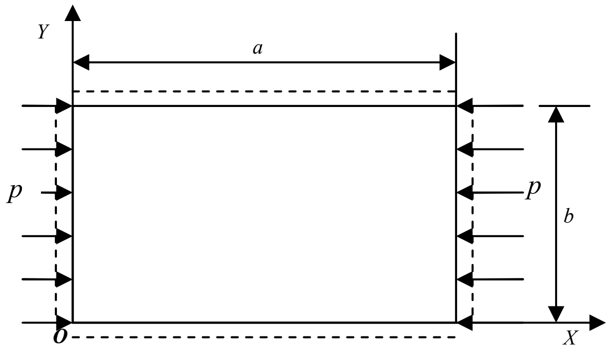

Fig. 1. Force sketch of plate neutral surface.

$$\frac{1}{D}\frac{Gh}{k_\tau}\frac{n\pi}{b}W_{mn}+\frac{1+\mu}{2}\frac{m\pi}{a}\frac{n\pi}{b}\Phi_{mn}+\frac{1-\mu}{2}(\frac{m\pi}{a})^2\Psi_{mn}+ (\frac{n\pi}{b})^2\Psi_{mn}+\frac{1}{D}\frac{Gh}{k_\tau}\Psi_{mn}=0 \tag{13b}$$

$$\frac{1}{D}\frac{Gh}{k_\tau}\frac{m\pi}{a}W_{mn}+(\frac{m\pi}{a})^2\Phi_{mn}+\frac{1-\mu}{2}(\frac{n\pi}{b})^2\Phi_{mn}+ \frac{1}{D}\frac{Gh}{k_\tau}\Phi_{mn}+\frac{1+\mu}{2}\frac{m\pi}{a}\frac{n\pi}{b}\Psi_{mn}=0 \tag{13c}$$

The relational expressions of Φ_{mn}, Ψ_{mn}, and W_{mn} can be obtained by the addition and subtraction of Eqs. (13b-13c):

$$\Phi_{mn}=\frac{W_{mn}}{D}\frac{Gh}{k_\tau}\frac{\Delta_1}{\Delta},\quad \Psi_{mn}=\frac{W_{mn}}{D}\frac{Gh}{k_\tau}\frac{\Delta_2}{\Delta} \tag{14a,b}$$

...where:

$$\Delta=-(1-\mu)(\frac{m\pi}{a})^2(\frac{n\pi}{b})^2-\frac{1-\mu}{2}(\frac{m\pi}{a})^4-\frac{1-\mu}{2}(\frac{n\pi}{b})^4 -\frac{3-\mu}{2}[(\frac{m\pi}{a})^2+(\frac{n\pi}{b})^2]\frac{1}{D}\frac{Gh}{k_\tau}-(\frac{1}{D}\frac{Gh}{k_\tau})^2 \tag{15a}$$

$$\Delta_1=\frac{1-\mu}{2}(\frac{m\pi}{a})^3+\frac{1-\mu}{2}\frac{m\pi}{a}(\frac{n\pi}{b})^2+\frac{1}{D}\frac{Gh}{k_\tau}\frac{m\pi}{a} \tag{15b}$$

$$\Delta_2=\frac{1-\mu}{2}(\frac{m\pi}{a})^2\frac{n\pi}{b}+\frac{1-\mu}{2}(\frac{n\pi}{b})^3+\frac{1}{D}\frac{Gh}{k_\tau}\frac{n\pi}{b} \tag{15c}$$

Eq. (15) is substituted into Eq. (14a):

$$W_{mn}\{\frac{Gh}{k_\tau}[(\frac{m\pi}{a})^2+(\frac{n\pi}{b})^2]+\frac{Gh}{k_\tau}[\frac{m\pi}{a}\frac{1}{D}\frac{Gh}{k_\tau}\frac{\Delta_1}{\Delta}+ \frac{n\pi}{b}\frac{1}{D}\frac{Gh}{k_\tau}\frac{\Delta_2}{\Delta}]-p(\frac{m\pi}{a})^2\}=0 \tag{16}$$

Two possibilities make the equation come into existence: there is a trivial solution with $W_{mn}=0$, i.e. the plates maintain the balance of plane state subjected to any load; for the untrivial solution of W_{mn}, the parentheses item should equal zero, that is:

$$p=\frac{a^2}{m^2}\frac{Gh}{k_\tau}\{[\frac{m^2}{a^2}+\frac{n^2}{b^2}]+\frac{1}{\pi D}\frac{Gh}{k_\tau}[\frac{m}{a}\frac{\Delta_1}{\Delta}+\frac{n}{b}\frac{\Delta_2}{\Delta}]\} \tag{17}$$

The buckling load means the minimum load satisfying Eq. (17). Based on the observation and analysis, it is considered that p monotonously increases with the growth of parameter n, so only one half-wave can be formed in the y direction (n=1). According to the extremum condition of function, the formula of $dp/dm=0$ is adopted to work out the minimal value of p with condition of $m=a/b$ (the parameter m must be a positive integer and discontinuous variable). The static balance method and dimensionless parameter of $P^*=pb^2/p^2D$ are adopted in the actual analysis, and the Matlab software is used to obtain the changing curves of $P^*= a/b$.

Solving and Curves of Critical Buckling Load

The buckling characteristics of simply supported rectangular medium plate are discussed, and the physical parameters are, respectively: $G=E/[2(1+\mu)]$, $D=Eh^3/[12(1-\mu^2)]$, $K=Eh/(1-\mu^2)$, $E=2.06\times10^5$MPa, μ=0.3, b=1,000 mm, and k_τ=5/6, n=1. The curves (Y-axis is pb^2/π^2D, X-axis is a/b) and corresponding data are given with conditions of $h=b/100$, $b/50$, $b/20$, $b/10$, $b/5$, $b/4$.

It can be seen from Figs. 2-7 and Table 1 that the dimensionless critical load P^* decreases with the increase of thickness h, the maximum and minimum values of which are about 4 and 3, respectively, showing that the buckling critical load of rectangular medium plate is less than that of thin plate for the energy consumption of transverse shear deformation. When the value of a/b is small,

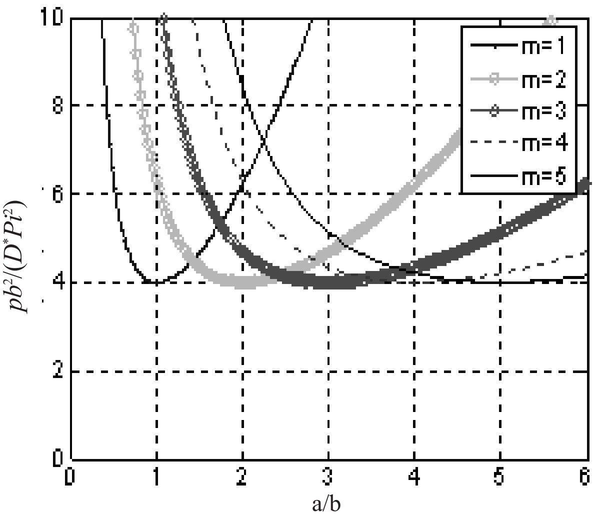

Fig. 2. Curves of $h=b/100$.

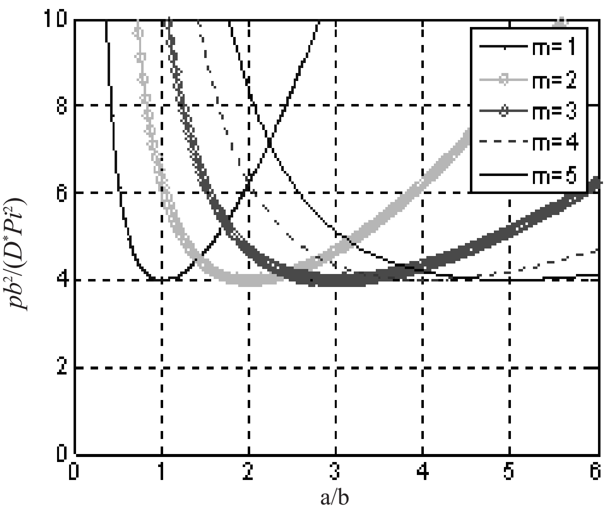

Fig. 3. Curves of $h=b/50$.

Table 1. Critical loading coefficient of the buckling of simply supported rectangular medium plates ($P^{*}=p_{cr}b^{2}/\pi^{2}D$).

Thickness	*a/b*=1	*a/b*=2	*a/b*=3	*a/b*=4	*a/b*=5
h=*b*/100	3.9981	3.9981	3.9981	3.9981	3.9981
h=*b*/50	3.9925	3.9925	3.9925	3.9925	3.9925
h=*b*/20	3.9535	3.9535	3.9535	3.9535	3.9535
h=*b*/10	3.8204	3.8204	3.8204	3.8204	3.8204
h=*b*/5	3.367	3.367	3.367	3.367	3.367
h=*b*/4	3.0918	3.0918	3.0918	3.0918	3.0918

the change of P^{*} with length-width ratio is particularly evident; when *a/b* >4, the change of P^{*} tends to be gentle. The critical load of rectangular medium plate is identical to the results obtained by theory of thin plate under the conditions of *h*=*b*/100, *b*/50, *b*/20, and now the displacement governing differential equations of the buckling of medium plates can degenerate to the corresponding displacement governing equations of thin plates, demonstrating the validity and generality of the solving process in this paper.

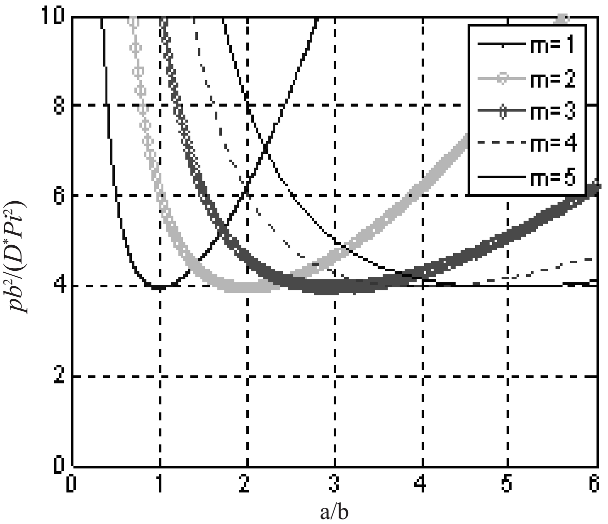

Fig. 4. Curves of *h*=*b*/20.

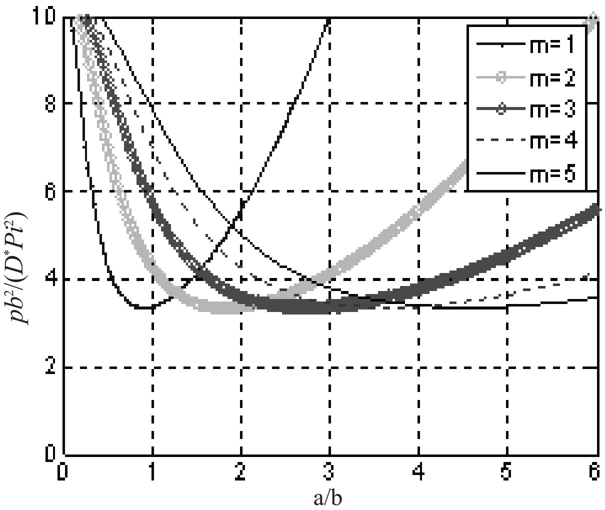

Fig. 6. Curves of *h*=*b*/5.

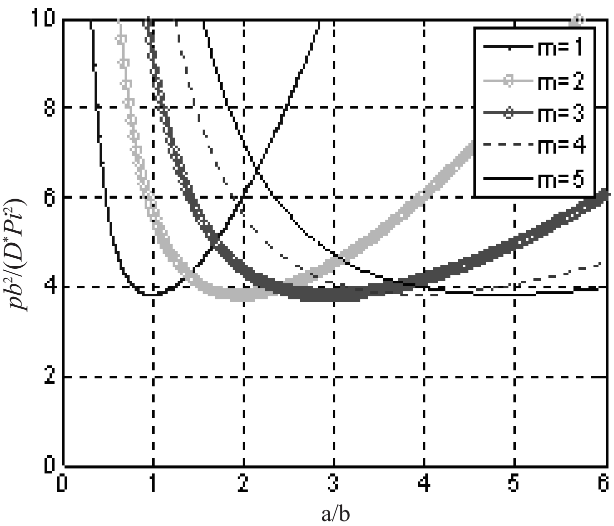

Fig. 5. Curves of *h*=*b*/10.

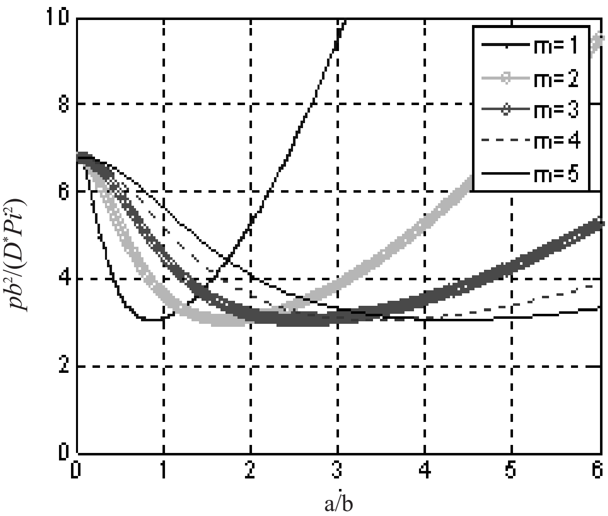

Fig. 7. Curves of h=b/4.

Post-Buckling Behavior of Rock Mass with Sheet Slope Crack

Displacement Governing Differential Equations of the Post-Buckling of Medium Plates

As a general rule, the buckling analysis of slope in geotechnical engineering only gives the critical load in a small stability range of ideal rock mass (classic load), but a lot of experimental studies show that the structure usually still has certain bearing capacity, producing corresponding deformation after buckling, and the failure load is often higher than the classical load. The elastic post-buckling behavior of plates and shells is also known as the supercritical form of plates and shells. The nonlinear large-deflection buckling theory provided by Karman and Hsue-shen Tsien is adopted in the post-buckling analysis of medium plates, which is based on geometric nonlinearity. The nonlinear partial differential governing equations of large-deflection buckling of rectangular medium plates without action of normal load are [14]:

$$\frac{1-\mu}{2}\frac{\partial^2\psi}{\partial x^2}+\frac{1+\mu}{2}\frac{\partial^2\phi}{\partial x\partial y}+\frac{\partial^2\psi}{\partial y^2}-\frac{1}{D}[\frac{Gh}{k_\tau}(\psi+\frac{\partial w}{\partial y})]=0 \quad (18a)$$

$$\frac{\partial^2\phi}{\partial x^2}+\frac{1-\mu}{2}\frac{\partial^2\phi}{\partial y^2}+\frac{1+\mu}{2}\frac{\partial^2\psi}{\partial x\partial y}-\frac{1}{D}[\frac{Gh}{k_\tau}(\phi+\frac{\partial w}{\partial x})]=0 \quad (18b)$$

$$\left[\frac{\partial\phi}{\partial x}+\frac{\partial\psi}{\partial y}+\frac{\partial^2 w}{\partial x^2}+\frac{\partial^2 w}{\partial y^2}\right]+\frac{k_\tau}{G}L(w,F)=0 \quad (18c)$$

$$\frac{1}{E}\nabla^2\nabla^2 F=(\frac{\partial^2 w}{\partial x\partial y})^2-\frac{\partial^2 w}{\partial x^2}\frac{\partial^2 w}{\partial y^2} \quad (18d)$$

...where $F(x,y)$ is the incoming stress function, and make:

$$\sigma_x=\frac{\partial^2 F}{\partial y^2},\sigma_y=\frac{\partial^2 F}{\partial x^2},\tau_{xy}=-\frac{\partial^2 F}{\partial x\partial y} \quad (19)$$

$L(w,F)$ is the differential operator:

$$L(w,F)=\frac{\partial^2 w}{\partial y^2}\frac{\partial^2 F}{\partial x^2}+\frac{\partial^2 w}{\partial x^2}\frac{\partial^2 F}{\partial y^2}-2\frac{\partial^2 w}{\partial x\partial y}\frac{\partial^2 F}{\partial x\partial y} \quad (20)$$

Eq. (18d) is the equation of strain compatibility obtained by the continuity condition of plane strain between membrane force and deflection in middle plane. The variables w, φ, ψ and stress function $F(x, y)$ can be worked out.

Post-Buckling of Simply Supported Rectangular Medium Plates with Unidirectional Pressure

According to the problem-solving ideas of Section 2, Eq. (12) is substituted into Eq. (18), and the relational expressions of Φ_{mn}, Ψ_{mn}, and W_{mn} can be obtained:

$$\Phi_{mn}=\frac{W_{mn}}{D}\frac{Gh}{k_\tau}\frac{\Delta_{mn1}}{\Delta_{mn}},\quad \Psi_{mn}=\frac{W_{mn}}{D}\frac{Gh}{k_\tau}\frac{\Delta_{mn2}}{\Delta_{mn}} \quad (21)$$

...where:

$$\Delta_{mn}=-(1-\mu)(\frac{m\pi}{a})^2(\frac{n\pi}{b})^2-\frac{1-\mu}{2}(\frac{m\pi}{a})^4-\frac{1-\mu}{2}(\frac{n\pi}{b})^4-\frac{3-\mu}{2}[(\frac{m\pi}{a})^2+(\frac{n\pi}{b})^2]\frac{1}{D}\frac{Gh}{k_\tau}-(\frac{1}{D}\frac{Gh}{k_\tau})^2 \quad (22a)$$

$$\Delta_{mn1}=\frac{1-\mu}{2}(\frac{m\pi}{a})^3+\frac{m\pi(1-\mu)}{2a}(\frac{n\pi}{b})^2+\frac{Ghm\pi}{Dk_\tau a} \quad (22b)$$

$$\Delta_{mn2}=\frac{1-\mu}{2}(\frac{m\pi}{a})^2\frac{n\pi}{b}+\frac{1-\mu}{2}(\frac{n\pi}{b})^3+\frac{1}{D}\frac{Gh}{k_\tau}\frac{n\pi}{b} \quad (22c)$$

When m=n=1 the complete solution of stress function can be obtained using the in-plane boundary condition of $\sigma_{xa}=\frac{1}{ah}\int_0^a pdy$ (σ_{xa} is the average pressure on the edges of x=0, a):

$$F=\frac{W_{11}^2E}{32}\left[\left(\frac{a}{b}\right)^2\cos\frac{2\pi}{a}x+\left(\frac{b}{a}\right)^2\cos\frac{2\pi}{b}y\right]-\sigma_{xa}\frac{y^2}{2} \quad (23)$$

Eq. (23) is substituted into Eq. (18c), the result solved by the Galerkin method with weight function of $\sin\frac{\pi}{a}x\sin\frac{\pi}{b}y$ can be obtained:

$$\sigma_{xa}=\frac{1}{h}\frac{a^2}{\pi^2}\left[\frac{Gh}{k_\tau}\left(\frac{\pi^2}{a^2}+\frac{\pi^2}{b^2}\right)+\frac{1}{D}\left(\frac{Gh}{k_\tau}\right)^2\frac{\pi}{a}\frac{\Delta_{111}}{\Delta_{11}}+\frac{1}{D}\left(\frac{Gh}{k_\tau}\right)^2\frac{\pi}{b}\frac{\Delta_{112}}{\Delta_{11}}\right]+\frac{\pi^2EW_{11}^2}{16}\left(\frac{1}{a^2}+\frac{a^2}{b^4}\right)=\sigma_{cr}+\frac{\pi^2EW_{11}^2}{16}\left(\frac{1}{a^2}+\frac{a^2}{b^4}\right) \quad (24)$$

...where σ_{cr} is the critical stress of small-deflection buckling, and the corresponding load expression can be obtained:

$$p=\frac{Gh}{k_\tau}[(1+\frac{a^2}{b^2})+\frac{a}{\pi}\frac{1}{D}\frac{Gh}{k_\tau}(\frac{\Delta_{111}}{\Delta_{11}}+\frac{a}{b}\frac{\Delta_{112}}{\Delta_{11}})]+\frac{EW_{11}^2}{16}\pi^2h(\frac{1}{a^2}+\frac{a^2}{b^4})=p_{cr}+\frac{EW_{11}^2}{16}\pi^2h(\frac{1}{a^2}+\frac{a^2}{b^4}) \quad (25)$$

...where p_{cr} is the critical load of small-deflection buckling.

Table 2. Critical loading coefficient of the post-buckling of simply supported rectangular medium plates ($P^*=p_{cr}b^2/\pi^2D$).

Thickness	a/b=0.2	a/b=0.4	a/b=0.6	a/b=1	a/b=1.4
$h=b/50$	26.3949	8.3531	5.1196	3.9925	4.4639
$h=b/20$	23.4571	8.0664	5.0262	3.9535	4.4309
$h=b/10$	16.7849	7.1858	4.7189	3.8204	4.3170
$h=b/5$	7.8516	5.0016	3.7914	3.3670	3.9145
$h=b/4$	5.6116	4.0730	3.3044	3.0918	3.6587

Solving and Curves of Critical Load

The dimensionless parameter of $P^*=pb^2/p^2D$ is also introduced to make the change curves of $P^*– W_{11}/h$ by Matlab. The same physical parameters of Section 2 are adopted in the post-buckling analysis of simply supported rectangular medium plates. The curves (Y-axis is pb^2/p^2D, X-axis is W_{11}/h) and corresponding data are given with conditions of h= b/50, b/20, b/10, b/5, b/4.

It can be seen from Figs. 8-12 and Table 2 that the post-buckling characteristics of plate are gradually obvious with the growth of large-deflection, i.e., the larger the load is, the larger the deformation of plate can be; the deformation of plate increases with the growth of thickness under the same load; the dimensionless critical load P^* decreases with the increase of thickness h, also showing that the buckling critical load of rectangular medium plate is less than that of thin plate for the energy consumption of transverse shear

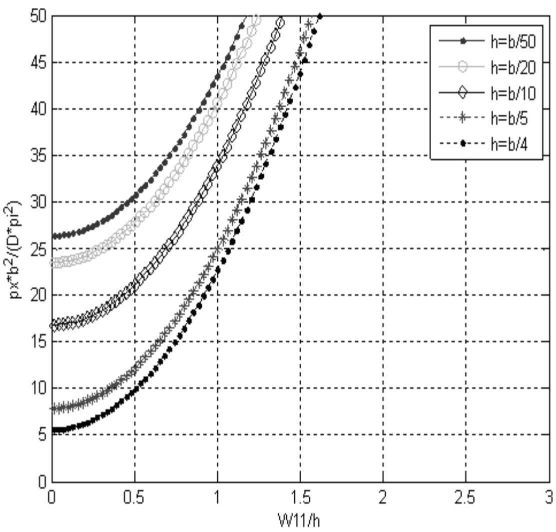

Fig. 8. Curves of a=0.2b.

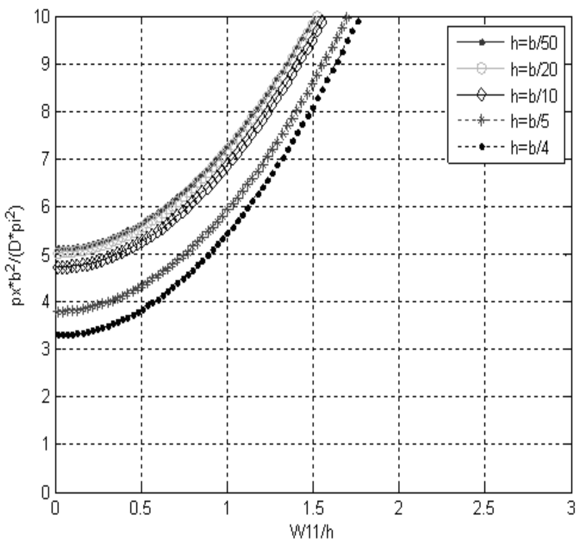

Fig. 10. Curves of a=0.6b.

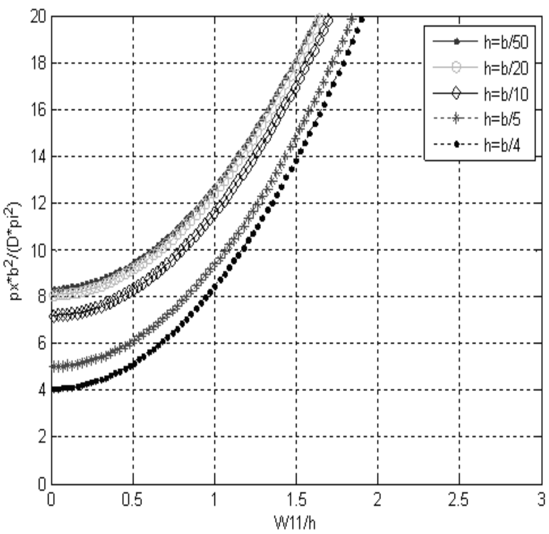

Fig. 9. Curves of a=0.4b.

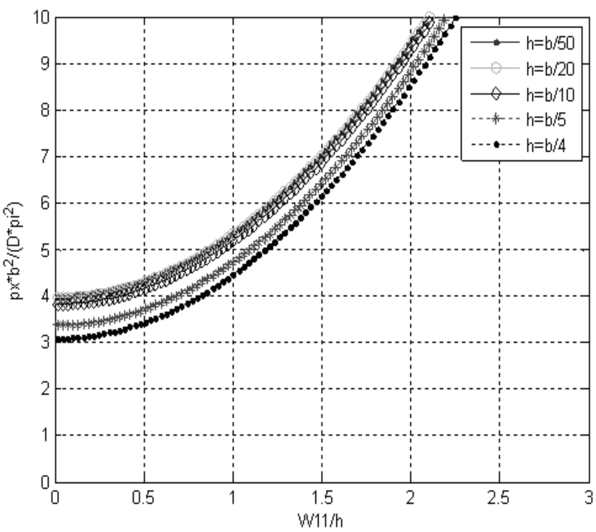

Fig. 11. Curves of a= b.

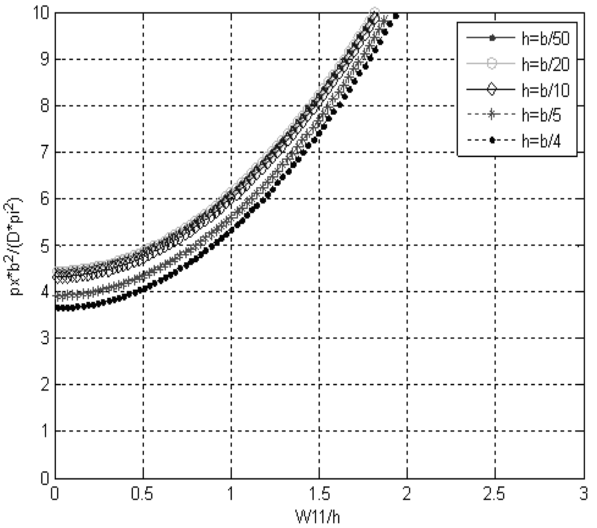

Fig. 12. Curves of *a*=1.4*b*.

deformation. The post-buckling characteristics of plate are different with the change of length-width ratio, and the dimensionless critical load of square plate (*a*=*b*) is the minimum. The critical load of rectangular medium plate is identical to the results obtained by the theory of thin plate under the conditions of *h*= *b*/50, *b*/20.

Verification of Hazardous Rock Mass in Slope

The hazardous rock mass of Zhenziyan is located at the eastern shoulder position oblique to the middle section of Jinfo Mountain. In the formation process of a steep cliff, the unloading and rebound are produced in the free face of rock mass, around which the principal stress trajectory has obvious deflection owing to the redistribution and differentiation of stress. The stress concentrated zone and maximum shear stress rising zone are produced respectively around the free face and slope toe, causing the suppression slip rupture face parallel to slope. The slope body rebounds toward free face with the action of unloading, causing the relaxation of original rock mass structure, the further deepening and increase of steep fracture, and the formation of unloading fissure zone.

The formation of steep cliff unloading fissure provides conditions for its time-dependent deformation failure. The weathering, softening, and disintegration of the limestone cemented with shale and argillaceous soil at the bottom of the steep cliff are produced under the actions of weathering, atmospheric precipitation, and groundwater to form a cavity, the further deformation of which is produced toward free face under the action of gravity from overlying rock mass, and the steep dip fissure zone is broken and expanded further. Thus, the steep cliff becomes a hazardous rock mass. After the formation of the hazardous rock, the buckling failures such as falling, dumping and slippage may appear under the action of outer dynamic factor.

The case study for the hazardous rock mass of Zhenziyan is progressed, and two groups of on-site test data are adapted for comparison and validation (Tables 3 and 4).

It can be seen from the above data that the extended length and expanded width both increase with the growth of length-width ratio (*a/b*), showing that the post-buckling characteristics of structure are more obvious. Meanwhile, the extended length and expanded width both increase with the diminution of thickness-width ratio (*h/b*). These regulations are basically accorded with the buckling and post-buckling characteristics of hazardous rock based on theory of plates and shells, demonstrating the validity and generality of the calculation results in this paper well.

Table 3. Comparison for the first group of dangerous rocks.

Elevation /m	**W18**	**W19**	Height ×width×height /m	**W18**	**W19**
	1605~1805	1605~1805		200×50×3	200×60×1
Main avalanche direction	**W18**	**W19**	Attitude of rocks	**W18**	**W19**
	200°	200°		300°∠5°	300°∠5°
Movement distance /m	**W18**	**W19**	Shape of hazardous rock	**W18**	**W19**
	600~2100	600~2100		sheet	sheet
Photographs of structure	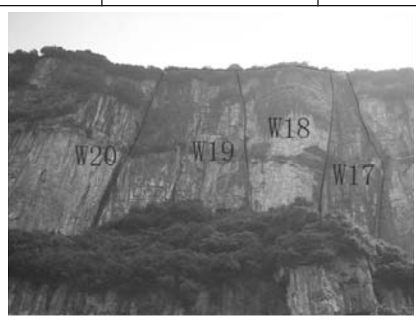				

Table 4. Comparison for the second group of dangerous rocks.

<table>
<tr><td rowspan="2">Elevation /m</td><td>W25</td><td>W26</td><td rowspan="2">Height ×width ×height /m</td><td>W25</td><td>W26</td></tr>
<tr><td>1404~1504</td><td>1620~1670</td><td>100×30×2</td><td>100×25×3</td></tr>
<tr><td rowspan="2">Main avalanche direction</td><td>W25</td><td>W26</td><td rowspan="2">Attitude of rocks</td><td>W25</td><td>W26</td></tr>
<tr><td>130°</td><td>145°</td><td>300°∠5°</td><td>300°∠5°</td></tr>
<tr><td rowspan="2">Movement distance /m</td><td>W25</td><td>W26</td><td rowspan="2">Shape of hazardous rock</td><td>W25</td><td>W26</td></tr>
<tr><td>500</td><td>300~1900</td><td>sheet</td><td>sheet</td></tr>
<tr><td rowspan="2">Photographs of structure</td><td colspan="5">W25

</td></tr>
<tr><td colspan="5">W26

</td></tr>
</table>

Conclusions

The rock mass with sheet slope crack is abstracted as sheet or medium plate, and some corresponding conclusions of the analytical solution based on theory of plates and shells can be obtained: the buckling critical load of rectangular medium plate is less than that of thin plate for the energy consumption of transverse shear deformation. When the value of a/b is small, the change of P^* with length-width ratio is particularly evident; when $a/b>4$, the change of P^* tends to be gentle. The critical load of rectangular medium plate is identical to the results obtained by theory of thin plate under the conditions of $h= b/100$, $b/50$, $b/20$.

The post-buckling characteristics of plate are gradually obvious with the growth of large-deflection, i.e., the larger the load is, the larger the deformation of plate is; the deformation of plate increases with the growth of thickness h under the same load; the dimensionless critical load P^* decreases with the increase of thickness h, also showing that the buckling critical load of rectangular medium plate is less than that of the thin plate for the energy consumption of transverse shear deformation. The post-buckling characteristics of plate are different with the change of length-width ratio, and the dimensionless critical load of square plate ($a=b$) is the minimum. The critical load of rectangular medium plate is identical to the results obtained by theory of thin plate under the conditions of $h= b/50$, $b/20$ demonstrating the generality of the analytical solution to provide a basis for the stability analysis of different slope hazardous rocks.

The shortcomings of this study include that all the solutions are built in the elastic range without the analysis for the plastic mechanical behaviors of plate, and only the load-carrying condition of the single plate in sheet crack is analyzed, so the analytical solution has certain limitations.

Acknowledgements

This work was supported by the National Basic Research Program of China (2013CB036000), the State Key Program of National Natural Science of China (No. 51139004). Great appreciation goes to the editorial board and the reviewers of this paper.

References

1. SUN G. Rock structural mechanics. Beijing: Science Press. **1988**.
2. HUDSON J. A., HARRISON J. P. Engineering rock mechanics (FENG Xia-ting & LI Xiao-chun, Trans.). Beijing: Science Press. **2009**.
3. ZHU Y., MUO H. On critical length of flexural slumping rock layer in layered rocky slope and its influencing factors. Rock and Soil Mechanics,. **25**, (2), 283, **2004**.
4. ZHU H., MA M., SHANG Y. Analysis of buckling failure of consequent rock slope. Journal of Zhejiang University, **38**, (9), 1144, **2004**.
5. ZHANG H. Post-buckling behavior of rock mass slope with sheet crack. Journal of Hunan University of Science & Technology (Natural Science Edition), **22**, (4), 73, **2007**.
6. LIU Y., HUANG R., DENG H. Study on physical simulation vibration test of the anti-inclined slab-rent structure rock slope. Journal of Chengdu University of Technology (Science & Technology Edition), **38**, (4), 413, **2011**.
7. WU L. Theory of Plates and Shells. Shanghai: Shanghai Jiaotong University Press. **1989**.
8. WU L. Stability Theory of Plates and Shells. Wuhan: Huangzhong keji University Press. **1996**.
9. HE F., SHENG Y. Theory of Plates and Shells. Xi'an : Xi'an Jiaotong University Press. **1993**.
10. CLIVE. L. DYM. Introduction to the Theory of Shells. New York: Pergamon Press. **1974**.
11. SHEN H. Post-buckling Behavior of Plates and Shells. Shanghai: Shanghai Press of Science and Technology. **2002**.
12. HUANG H., HAO J., HUANG Y. Displacement fundamental equations o f the thick plates bending and the general solution to simply supported rectangular plates by transverse shearing deformation. J. Xi'an University of Architecture & Technology (Natural Science Edition), **41**, (6), 780, **2009**.
13. HUANG H., HAO J., ZHANG H., GUO J. Study on buckling of simply supported rectangular medium plate considering the transverse shearing deformation. J. Xi'an University of Architecture & Technology (Natural Science Edition), **43**, (5), 638, **2011**.
14. HUANG H., HAO J., ZHANG H. Study on post-buckling of moderately thick rectangular plates considering transverse shearing deformation. Chinese Quarterly of Mechanics, **31**, (4), 618, **2010**.